

2022

Recent advances in luminescence and lasing research in ZBYA glass

Changjun Xu

Jiquan Zhang

Mo Liu

See next page for additional authors

Follow this and additional works at: <https://arrow.tudublin.ie/prcart>



Part of the [Electrical and Computer Engineering Commons](#)

This Article is brought to you for free and open access by the Photonics Research Centre at ARROW@TU Dublin. It has been accepted for inclusion in Articles by an authorized administrator of ARROW@TU Dublin. For more information, please contact arrow.admin@tudublin.ie, aisling.coyne@tudublin.ie, gerard.connolly@tudublin.ie.






This work is licensed under a [Creative Commons Attribution-NonCommercial-Share Alike 4.0 License](#)
Funder: National Natural Science Foundation of China (61905048, 61935006, 62005060, 62005061, 62090062); Heilongjiang Provincial Natural Science Foundation (LH2020F030); National Key Research and Development Program of China (2020YFA0607602); Shenzhen BasicResearch Foundation (JCYJ20190808140805488, JCYJ20190808173619062); 111 Project (B13015); Heilongjiang Touyan Innovation Team Program; Fundamental Research Funds for the Central Universities (3072021CF2514, 3072021CF2533).

Authors

Changjun Xu, Jiquan Zhang, Mo Liu, Haiyan Zhao, Fengzi Ling, Shijie Jia, Gerald Farrell, Shunbin Wang, and Pengfei Wang



Recent advances in luminescence and lasing research in ZBYA glass

CHANGJUN XU,¹ JIQUAN ZHANG,¹  MO LIU,¹  HAIYAN ZHAO,²
FENGZI LING,² SHIJIE JIA,¹ GERALD FARRELL,³ SHUNBIN
WANG,^{1,4} AND PENGFEI WANG^{1,2,*} 

¹Key Laboratory of In-Fiber Integrated Optics, Ministry Education of China, Harbin Engineering University, Harbin 150001, China

²Key Laboratory of Optoelectronic Devices and Systems of Ministry of Education and Guangdong Province, College of Optoelectronic Engineering, Shenzhen University, Shenzhen, 518060, China

³Photonics Research Center, Technological University Dublin, Grangegorman Campus, Dublin 7, Ireland

⁴shunbinwang@hrbeu.edu.cn

*pengfei.wang@tudublin.ie

Abstract: In the last few decades, fluoride glasses have attracted a growing interest due to their unique advantages compared to multi-component oxide glasses. Among them, the most studied and widely used were fluorozirconate glasses, represented by $\text{ZrF}_4\text{-BaF}_2\text{-LaF}_3\text{-AlF}_3\text{-NaF}$ (ZBLAN) glasses. However, compared with ZBLAN glasses, a kind of fluorozirconate glass with the components $\text{ZrF}_4\text{-BaF}_2\text{-YF}_3\text{-AlF}_3$ (ZBYA) has higher thermal and chemical stability. In this paper, we first introduce the advantages of ZBYA glasses compared to ZBLAN glasses. Then we review and discuss recent advances in research on luminescence and lasing in ZBYA glass and fiber. These studies suggest that ZBYA glass has strong potential for use as a gain medium material in high power mid-infrared fiber lasers.

© 2022 Optica Publishing Group under the terms of the [Optica Open Access Publishing Agreement](#)

1. Introduction

In 1961, Snitzer first reported lasing in a Nd^{3+} doped barium crown glass, proving that the glass material can be used as laser gain medium material [1]. Since then, laser gain glass has been developed rapidly. Compared with crystalline materials, laser gain glass has been widely used in many applications such as solid-state lasers and glass fiber lasers because of its reliance on simple and mature fabrication methods, adjustable glass components, good optical quality and optical uniformity. Oxide glasses, due to their good chemical stability and mechanical properties, have attracted great attention and have been widely studied [2–6]. However, the high phonon energy of oxide glass results in a higher probability of non-radiative mechanisms in rare-earth (RE) doped glasses, which restricts their use in applications involving luminescence.

Fluoride glass is a non-oxide glass, which has low phonon energy (as low as 510 cm^{-1}), a broad transparency range ($0.22\text{ }\mu\text{m}$ – $7\text{ }\mu\text{m}$) and can tolerate relatively high doping levels (up to 10%). The discovery of fluorozirconate glasses in the 1970s [7], resulted substantial research efforts in the areas of luminescent materials and infrared optical devices using such glasses. Research on fluoride glasses mainly focuses on fluorozirconate glasses, fluoroaluminate glasses and fluoroindate glasses. In particular, fluorozirconate glasses, represented by ZBLAN glasses, has been intensively studied, given its wide transmission window and low phonon energy. However, ZBLAN glasses have very poor chemical and thermal stability, resulting in a degradation in the optical performance limiting its use in real-world applications. It is crucial therefore to investigate glass materials which simultaneously combine good optical properties with high thermal and chemical stability.

In 1984, a form of novel fluorozirconate glasses with the components $\text{ZrF}_4\text{-BaF}_2\text{-YF}_3\text{-AlF}_3$ was reported by Vaughn and Risbud for the first time [8]. Compared with ZBLAN glasses, the

NaF component was removed, as it readily absorbs water and YF_3 , which has a higher melting point, was introduced. ZBYA glasses are therefore theoretically more chemically stable and possess a higher glass transition temperature (T_g) and crystallization temperature (T_x). It is not surprising then that the optical properties of ZBYA glasses have been extensively studied.

In this paper, the properties of ZBYA glasses and ZBLAN glasses are presented in Section 2. The thermal and chemical properties of these two types of fluorozirconate glasses are then compared. Then in Section 3, recent research progress in our laboratory on ZBYA fluorozirconate glasses and fibers is reviewed and discussed. These experimental results demonstrate that ZBYA glass material has good optical properties, a high rare-earth solubility and low phonon energy; therefore, it has great potential for application in the fiber lasers.

2. Synthesis and properties of ZBYA glasses

ZBYA glass, given its low phonon energy, wide transmission window, and improved stability make it an excellent gain medium material in the mid-infrared region where emissions are challenging to obtain from silicate and oxide glasses [9,10]. However, to be useful as gain medium in optical fiber lasing applications, there are a series of specific parameters for optical glasses which are critical, such as the glass transition temperature, thermal and chemical stability, transmission spectral range and maximum phonon energy. In this section, we briefly discuss the synthesis of ZBYA glasses and basic physical characterizations of ZBYA glass materials are also summarized in this section.

2.1. ZBYA glass synthesis

The fabrication of ZBYA glass is performed using a conventional melt quenching method. In our experiments, raw materials powders with a purity of more than 99.9% were fully mixed with the molar ratio of $50\text{ZrF}_4\text{-}33\text{BaF}_2\text{-}10\text{YF}_3\text{-}7\text{AlF}_3$. The mixing of the materials is carried out in a nitrogen-filled glove box to avoid contamination by air and moisture. Then, the mixed samples were added into platinum crucibles and heated in a muffle furnace at $850\text{ }^\circ\text{C}$ for 2 h. The completely molten high-temperature glass liquid was poured onto a copper plate preheated at $320\text{ }^\circ\text{C}$ and annealed in a muffle furnace for 3 h to eliminate glass stress. The liquid was then naturally cooled to room temperature to obtain glass samples. The entire preparation was carried out in a glove box filled with dry nitrogen to eliminate hydroxyl contamination of the glasses.

2.2. Optical properties of ZBYA glass

The Raman spectrum and transmission spectrum over the range 200 nm – 10000 nm of the un-doped ZBYA glass sample are shown in Fig. 1. The peaks in the Raman spectrum are caused by lattice vibrations, and the maximum Raman shift peak is located at 571 cm^{-1} , which is attributed to the vibration of the Zr-F bond in the $[\text{ZrF}_6]$ octahedron. As result the maximum phonon energy of ZBYA glass can be determined as $\sim 570\text{ cm}^{-1}$, as confirmed by Fig. 1(a). The ZBYA glass also has a broad transparency range (200-9000 nm) and possesses outstanding transmittance (around 90%) over the range of 500-6000 μm due to its low phonon energy, as depicted in Fig. 1(b). The very slight absorption dip in the region around 3 μm is the result of residual OH^- vibrations in the glass. It can be concluded then that ZBYA glass has similar phonon energy and transparency range to ZBLAN glass, but to give ZBYA glass a decisive advantage in near and mid-infrared band applications, ZBYA glass needs to be able to demonstrate improved thermal and chemical stability compared to ZBLAN glass.

2.3. Thermal properties of ZBYA glass

The thermal stability of a glass is defined as the performance of a glass subjected to severe temperature changes without incurring catastrophic damage. Among the key thermal parameters

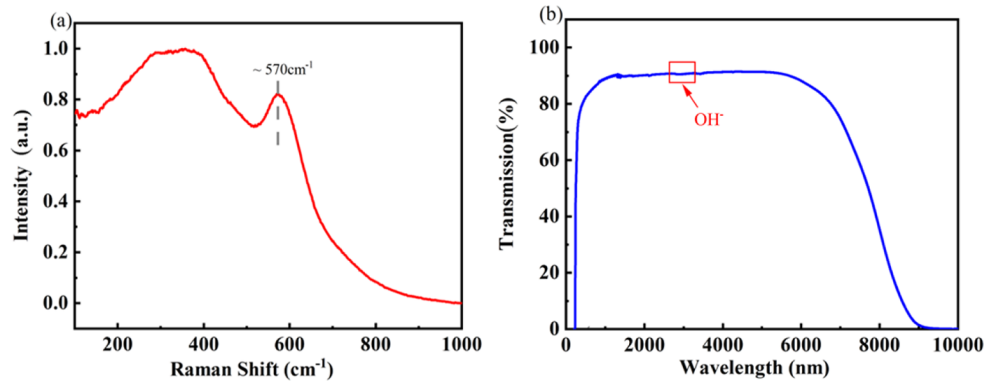


Fig. 1. (a) Raman spectrum of undoped ZBYA glass sample. (b) Transmission spectrum of the 2.0 mm thick ZBYA glass.

of glass, the glass transition temperature (T_g) is the characteristic temperature where the glass changes from the glassy state to the highly elastic state as a result of heating and the glass crystallization temperature (T_x) is the characteristic temperature where the glass begins to crystallize. Differential scanning calorimetry (DSC) was used to measure the T_g and T_x of ZBYA and ZBLAN glasses, as shown in Fig. 2. From this experiment, the T_g and T_x values of ZBYA glass are determined as 333 °C and 405 °C, which are 68 °C and 75 °C higher respectively, compared to ZBLAN glass.

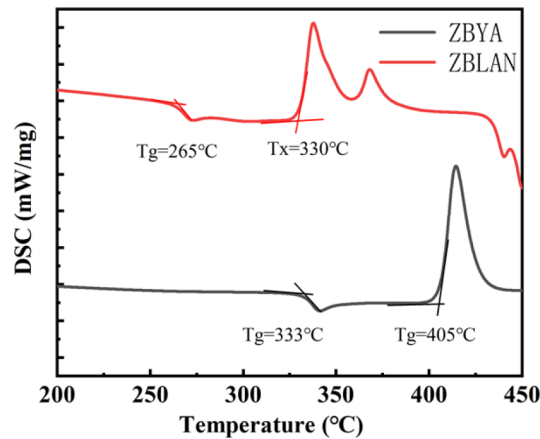


Fig. 2. DSC curves of ZBYA and ZBLAN glass samples and the characteristic temperature.

In addition to T_g and T_x , the figure-of-merit (R_s) parameter, sometimes called the shock resistance, is commonly used to quantify the thermal-mechanical properties of optical glass material. The R_s for glass materials is determined by thermal conductivity k , Poisson's ratio ν , coefficient of thermal expansion α , elastic modulus E , and fracture stress σ_F . The detailed formula is expressed as follows [11]:

$$R_s = \frac{k(1 - \nu)}{\alpha E} \sigma_F \quad (1)$$

The measured parameters and the calculated R_s of ZBYA glass are shown in Table 1. The calculated R_s of ZBYA glass is 0.197, which is larger than that of ZBLAN glass (0.138) [12].

The higher T_g of ZBYA glass means a higher laser damage resistance, and the larger R_s values indicate that ZBYA glass could be able to withstand stronger thermal shock rather than ZBLAN in high-power laser systems.

Table 1. Thermal and Mechanical parameters of ZBYA glass

K (W/m/K)	ν	α ($10^{-6}/K$)	E (Gpa)	σ_F (Mpa·m ^{1/2})	R_s (W·m ^{1/2})
0.61	0.22	19.4	55.9	0.45	0.197

2.4. Chemical stability of ZBYA glass

Understanding the chemical stability is also important for the prediction of the optical performance of fluoride glass. The chemical stability of fluorozirconate glasses is mainly reflected in their resistance to water erosion. In 2014, Tanya Moron et al. studied the chemical durability of fluorozirconate and fluoroindate glasses in deionized water [13]. Fluorozirconate glasses exhibit multi-layered hydrate of different compositions after immersion in water, resulting in a reduction in transmittance, especially at 2.9 μm and 6.1 μm band, attributed to the absorption of OH^- and OHO , respectively.

ZBYA glass and ZBLAN glass samples were subjected to water immersion experiments to study the chemical stability of ZBYA glass. The undoped ZBYA and ZBLAN glasses were polished and cut into samples with a size $10 \times 10 \times 1.4$ mm for subsequent measurements. Both glasses were immersed in deionized water for different durations (0 h, 12 h, 24 h), then dried in a muffle furnace with a nitrogen atmosphere at 100 °C for 12 hours. The transmittance spectra and weights of the samples of the two glass types for different immersion durations were recorded and are shown in Fig. 3. Before immersion, both glass types have a transmittance of around 90% over the range of 500-6000 μm . After reaction with water, both ZBLAN and ZBYA glasses showed a decrease in transmittance, and two strong absorption peaks occurred at 2.9 μm and 6.1 μm bands. However, the transmittance of ZBYA glass decreased less as a function of immersion duration compared to ZBLAN glass (See Fig. 3(a) and 3(b)), suggesting that the hydrolysis reaction of the ZBYA glass was slower. As shown in the comparison in Fig. 3(c), after 24 hours of immersion, ZBLAN glass is almost completely opaque, while ZBYA glass still has a transmittance of around 50% in the 4-6 μm band.

Both two glasses lost weight to varying degrees after drying, mainly due to the high solubility of ZrF_4 in water and the exchange of F^- and OH^- . However, it is known that the introduction of alkali glass modifiers to fluoride glasses (such as Li, Na and K) will increase their reaction rates [15–18], resulting in ZBLAN glass having a much higher weight loss than that of ZBYA glass, as shown in Fig. 3(d). These results suggest that the NaF-free ZBYA glass has better resistance to deliquescence, which provides for a longer working life in humid environments.

In summary, the characteristic parameters of ZBLAN glass and ZBYA glass are listed in Table 2.[19–22]. Consequently, ZBYA glasses may be considered a promising candidate for MIR optical applications.

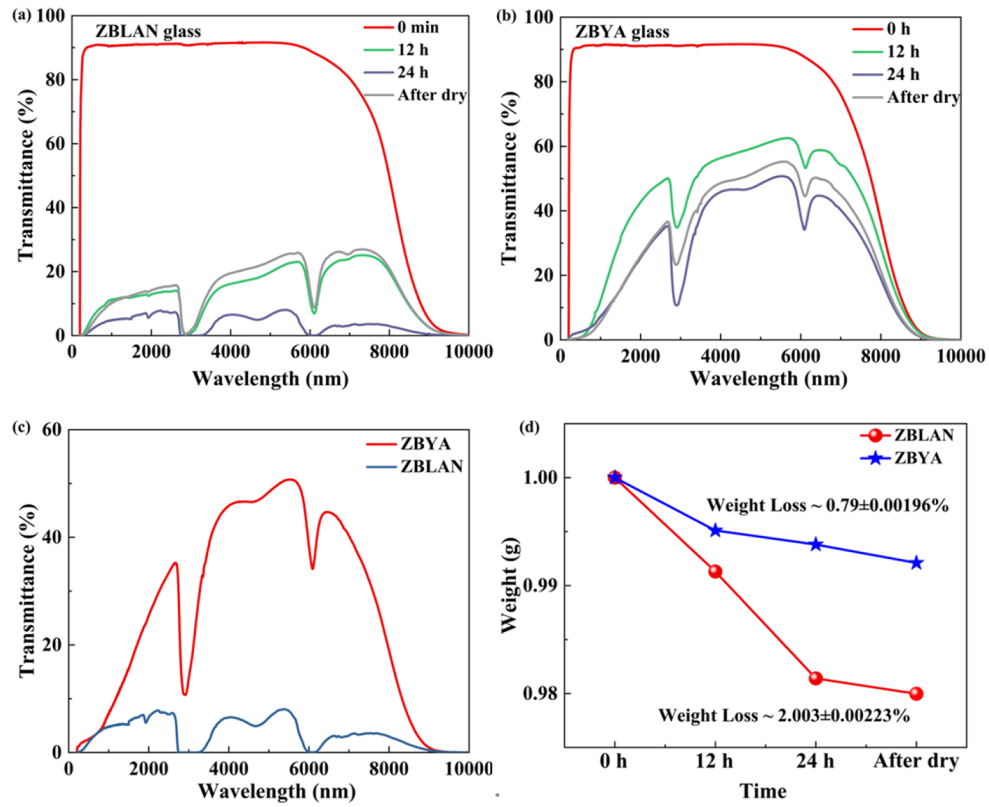


Fig. 3. Transmission spectrum of (a) ZBLAN and (b) ZBYA glasses after leaching in deionized for different time (c) Spectral comparison of ZBLAN and ZBYA glass samples after 24 h leaching in deionized (d) Loss of weight comparison of ZBLAN and ZBYA glass samples after leaching in deionized water [14].

Table 2. Comparison of basic properties between ZBLAN glass and ZBYA glass

Value	ZBLAN	ZBYA
Maximum phonon energy(cm^{-1})	~580	~571
Transmission range($T \approx 90\%$) (μm)	0.2-6	0.2-6
Transition temperature (T_g) ($^{\circ}\text{C}$)	265	333
Crystallization temperature (T_x) ($^{\circ}\text{C}$)	330	405
Thermal conductivity (W/m/K)	0.63	0.61
Poisson's ratio	0.31	0.22
Coefficient of thermal expansion ($10^{-6}/\text{K}$)	17.2	19.4
Elastic modulus (Gpa)	58.3	55.9
Fracture stress ($\text{Mpa}\cdot\text{m}^{1/2}$)	0.32	0.45
R_s , Figure-of-merit ($\text{W}\cdot\text{m}^{1/2}$)	0.138	0.197
Density (g/cm^3)	4.33	4.53
Refractive index (@ 589 nm)	1.499	1.504

3. Recent research based on ZBYA glass

3.1. MIR luminescence properties

ZBYA glass have recently attracted a lot of research interest because of its low phonon energy and excellent optical properties over the mid-infrared region. In 2013, Huang et al. studied the intensive fluorescence of 2.7 μm in highly Er^{3+} doped ZBYA glass and suggested that Er^{3+} doped ZBYA glass has potential application in 2.7 μm lasers [23]. They also investigated the energy transfer mechanism of $\text{Er}^{3+}/\text{Ho}^{3+}$, $\text{Er}^{3+}/\text{Pr}^{3+}$, $\text{Er}^{3+}/\text{Tm}^{3+}$ co-doped ZBYA glass to improve the $\lambda \sim 2.7 \mu\text{m}$ emission [24,25].

$\lambda \sim 2.9 \mu\text{m}$ MIR emission can be obtained from transition ${}^6\text{H}_{13/2} \rightarrow {}^6\text{H}_{15/2}$ level in Dy^{3+} ion, which is longer than that of $\text{Er}^{3+}: {}^4\text{I}_{11/2} \rightarrow {}^4\text{I}_{13/2}$ [26]. In 2020, we investigated and discussed the MIR emission in $\text{Dy}^{3+}/\text{Tm}^{3+}$ co-doped ZBYA glass under the excitation of an 808 nm laser diode and proved that the MIR fluorescence of Dy^{3+} can be effectively improved by introducing Tm^{3+} ions in ZBYA glass [27]. Figure 4 shows the luminescence spectra at $\lambda \sim 2.9 \mu\text{m}$ in different doping concentrations of $\text{Dy}^{3+}/\text{Tm}^{3+}$ co-doped ZBYA glass. Figure 4(a) shows that the 2.9 μm fluorescence intensity increases with increasing Dy^{3+} doping content with a fixed Tm^{3+} doping concentration of 1 mol.%, indicating an efficient energy transfer between $\text{Tm}^{3+}: {}^3\text{F}_4$ and $\text{Dy}^{3+}: {}^6\text{H}_{13/2}$ level. When the Dy^{3+} doping concentration is fixed, the fluorescence intensity at $\lambda \sim 2.9 \mu\text{m}$ increased gradually with the increase of Tm^{3+} concentration, as shown in Fig. 4(b).

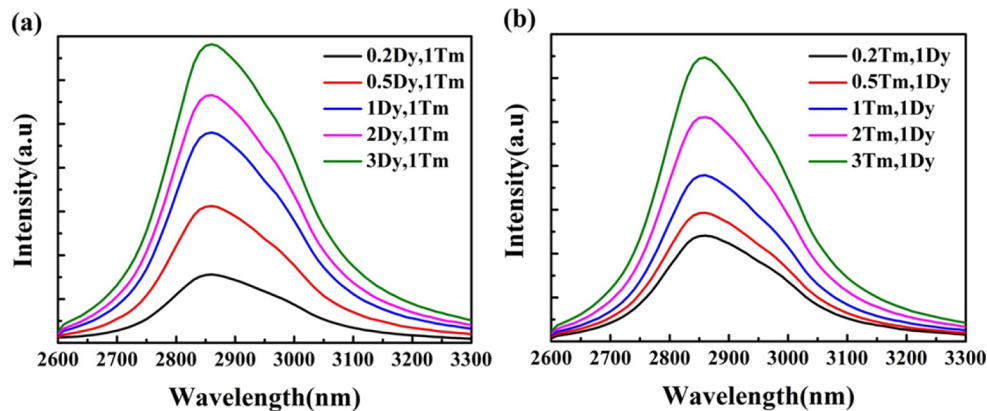


Fig. 4. Luminescence spectra of Dy^{3+} ions at the $\lambda \sim 2.9 \mu\text{m}$ wavelength in different doping concentrations (a) Fixed Tm^{3+} ion concentration of 1 mol. % (b) Fixed Dy^{3+} ion concentration of 1 mol. % [27].

Figure 5 displays the energy transfer processes in $\text{Dy}^{3+}/\text{Tm}^{3+}$ co-doped ZBYA glass. Firstly the transition ${}^6\text{H}_{15/2} \rightarrow {}^6\text{F}_{5/2}$ occurs under the excitation of an 808 nm laser and in addition Tm^{3+} ions in the ground state ${}^3\text{H}_6$ level are excited to the ${}^3\text{H}_4$ excited state level as a result of pumping by the 808 nm laser. The absorption efficiency of 808 nm by Dy^{3+} ions is enhanced according to the energy transfer (ET) processes $\text{Tm}^{3+}: {}^3\text{H}_4, {}^3\text{H}_5, {}^3\text{F}_4 \rightarrow \text{Dy}^{3+}: {}^6\text{F}_{5/2}, {}^6\text{F}_{11/2} ({}^6\text{H}_{9/2}), {}^6\text{H}_{11/2}$. The ions in the upper energy level are transmitted to the ${}^6\text{H}_{13/2}$ level through multi-phonon relaxation process (MPR) and accumulated at ${}^6\text{H}_{13/2}$ level, resulting in 2.9 μm mid-infrared emission.

To explore the potential of ZBYA glass in longer wavelength applications, we have fabricated ZBYA glasses with different Ho^{3+} doping concentrations (0.1, 0.2, 0.5, 1, 2, 3, 4, 5, 7, 9%) and MIR emission at $\lambda \sim 3.9 \mu\text{m}$ was demonstrated under 888 nm pump [28]. The luminescence spectra of the different wavelengths are shown in Fig. 6. It can be seen that the intensity of each emission rises with an increase in the Ho^{3+} doping concentration and that no concentration

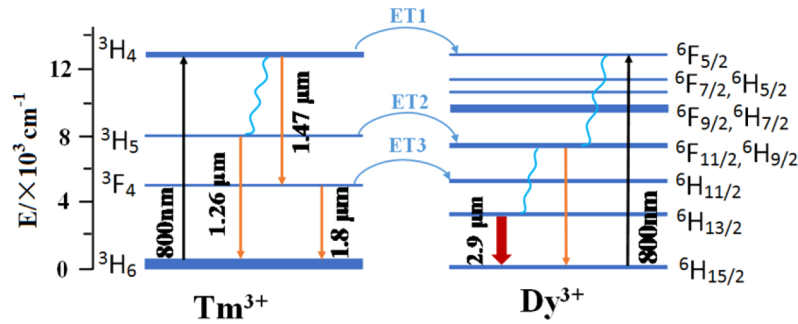


Fig. 5. Energy transfer processes of $\text{Dy}^{3+}/\text{Tm}^{3+}$ co-doped ZBYA glass [27].

quenching phenomenon occur. Several radiative parameters of Ho^{3+} doped ZBYA glass were calculated, including spontaneous radiation transition probabilities (A), fluorescence branching ratio (β), and the radiative lifetime (τ_{rad}) as shown in Table 3. ZBYA glass has a long radiative lifetime of 21.9 ms for ${}^5\text{I}_5 \rightarrow {}^5\text{I}_6$ transition, suggested a strong potential for 3.9 μm laser emission.

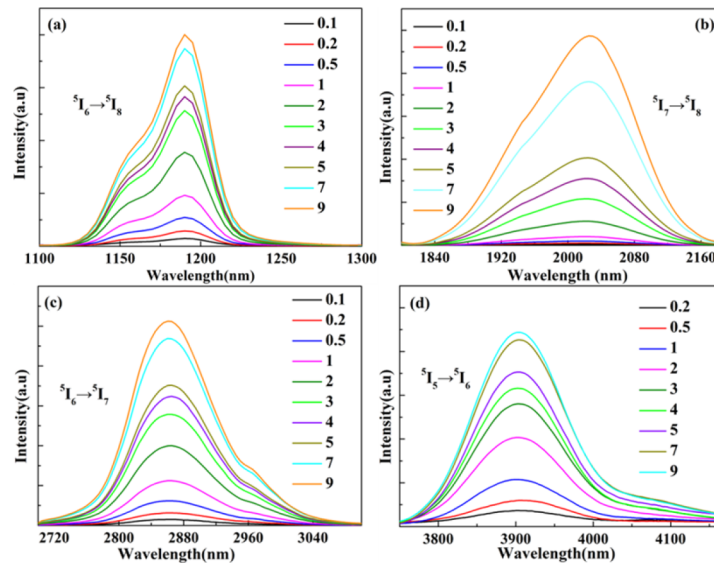


Fig. 6. Luminescence spectra of different doping concentration Ho^{3+} -doped ZBYA glass at (a) $\lambda \sim 1190$ nm, (b) $\lambda \sim 2010$ nm, (c) $\lambda \sim 2.9$ μm , and (d) $\lambda \sim 3.9$ μm wavelength [28].

Table 3. Radiative Property Parameters for Transitions between Various Energy Levels of Ho^{3+} in ZBYA Glass [28]

Transition	Wavelength (nm)	A (s^{-1})	β (%)	τ_{rad} (ms)
${}^5\text{I}_5 \rightarrow {}^5\text{I}_6$	3920	2.96	6.48	21.9
$\rightarrow {}^5\text{I}_7$	1640	26	56.95	
$\rightarrow {}^5\text{I}_8$	890	16.7	36.57	
${}^5\text{I}_6 \rightarrow {}^5\text{I}_7$	2860	6.26	9.3	14.8
$\rightarrow {}^5\text{I}_8$	1190	61.1	90.7	
${}^5\text{I}_7 \rightarrow {}^5\text{I}_8$	2010	22.76	100	43.9

In summary, efficient MIR emission can be realized in Er^{3+} , Dy^{3+} and Ho^{3+} ions doped ZBYA glass, indicating that ZBYA glass should be a good gain material for MIR lasers.

3.2. ZBYA microsphere laser based on the whispering gallery mode (WGM)

In recent years, microcavity resonators, including microsphere, microring, microdisk, and microroid etc, have attracted great attention because of their unique advantages, such as high-Quality factors (Q-factors), low threshold and narrow line-width output in laser applications [29–38]. Amongst several possible microcavities, a microsphere cavity has been studied most due to its advantages of high Q value ($\sim 10^8$), simple fabrication and good axial symmetry. Microsphere lasers have been demonstrated successfully in many glass materials [39–44]. Compared to silica glass and oxide glass, the chemical properties of fluorozirconate glass are not stable enough, and it is very easy to crystallize the glass during the heating process. Therefore, it is challenging to prepare high Q-value microspheres based on fluorozirconate.

ZBYA glass is a superior laser gain medium for a microsphere laser given its low phonon energy and broad transmission windows. In 2019, Er^{3+} doped ZBYA microspheres were fabricated from glass filaments, and multi and single-mode lasing at $1.56 \mu\text{m}$ was achieved under pumping by a 980 nm laser [45]. The experimental setup and measurement system is shown in Fig. 7, along with some microscope photos of the glass structures.

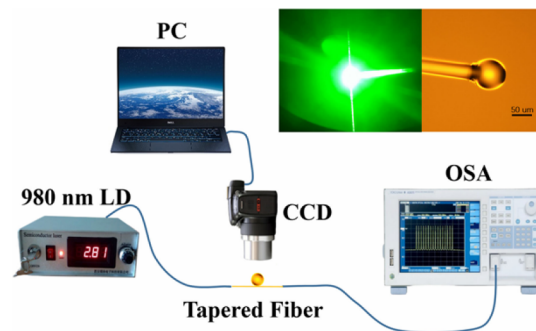


Fig. 7. Experiment setup for Er^{3+} doped ZBYA microsphere laser. Inset are the microscope photos of ZBYA microsphere [45].

The ZBYA microsphere was fabricated by reflowing the tip of a ZBYA glass fiber with a CO_2 laser. The ZBYA fiber tip was heated and melted by a CO_2 laser, then under the effect of gravity and surface tension, a ZBYA microsphere was formed. The microsphere diameter is $68 \mu\text{m}$, and the 980 nm laser was coupled to the Er^{3+} doped ZBYA microsphere using evanescent coupling from a tapered fiber. Laser emission at C-band was observed when the pump power was 1.34 mW. The laser spectrum is shown in Fig. 8. Figure 8(a) displays the multi-mode laser spectrum centered at $\lambda \sim 1.56 \mu\text{m}$ with a pump power of 14.2 mW. A single-mode laser output with an extremely narrow linewidth of 0.1 nm can be obtained by adjusting the coupling position between the tapered fiber and ZBYA microsphere, as shown in Fig. 8(b). This C-band laser emission in the ZBYA microsphere indicated that ZBYA glass might have potential applications in the optical communications area.

Lasers at wavelengths around $\lambda \sim 2.0 \mu\text{m}$ have attracted widespread interest because of their applications in medical surgery and lidar for eye safety. So, in order to explore the potential lasing applications of ZBYA glass over the wavelength range of $2 \mu\text{m}$, Tm^{3+} doped and $\text{Ho}^{3+}/\text{Tm}^{3+}$ co-doped ZBYA microsphere lasers were also investigated in 2019 and 2020, respectively [46,47]. The preparation of two ZBYA microspheres is similar to that of Er^{3+} -doped ZBYA microsphere. The Tm^{3+} doped and $\text{Ho}^{3+}/\text{Tm}^{3+}$ co-doped ZBYA microspheres were pumped by 808 nm and

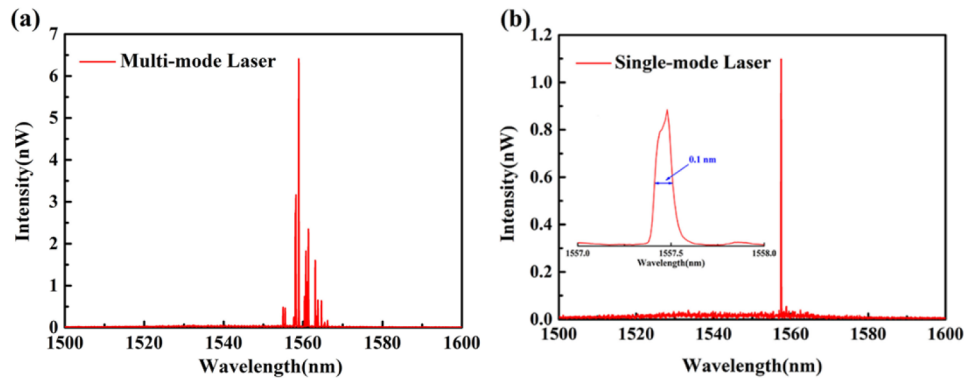


Fig. 8. Spectrum of (a) multi-mode laser and (b) single-mode laser in Er^{3+} doped ZBYA microsphere [45].

793 nm lasers, respectively. Multi and single wavelength laser emission was observed in the Tm^{3+} doped ZBYA microsphere. Figure 9 displays the laser spectrum of $\lambda \sim 2 \mu\text{m}$, the laser threshold as low as 5.6 mW and single-mode lasing at 1897 nm can be realized by adjusting the coupling position between the ZBYA microsphere and the silica fiber taper.

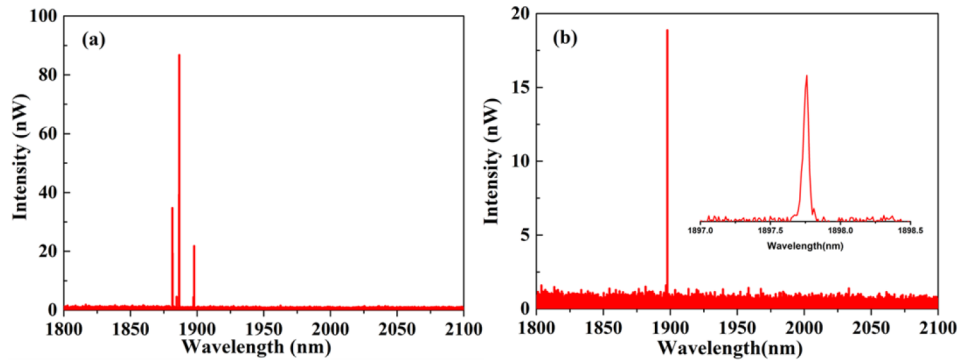


Fig. 9. Spectrum of (a) multi-mode laser and (b) single-mode laser in Tm^{3+} doped ZBYA microsphere [46].

For $\text{Ho}^{3+}/\text{Tm}^{3+}$ co-doped ZBYA microspheres, triple-wavelength laser operation at 1.5 μm , 1.8 μm and 2.0 μm was also obtained, which is attributed to the radiative transitions of Tm^{3+} : ${}^3\text{H}_4 \rightarrow {}^3\text{F}_4$, Tm^{3+} : ${}^3\text{F}_4 \rightarrow {}^3\text{H}_6$, and Ho^{3+} : ${}^5\text{I}_7 \rightarrow {}^5\text{I}_8$, respectively. In Tm^{3+} single-doped condition, lasing at 1.5 μm is hard to achieve as the ${}^3\text{H}_4 \rightarrow {}^3\text{F}_4$ transition includes self-terminating population inversion. The introduction of Ho^{3+} can decrease the population of Tm^{3+} : ${}^3\text{H}_4$, so that lasing emission at $\lambda \sim 1.50 \mu\text{m}$ is easier to achieve. The spectrum of $\text{Ho}^{3+}/\text{Tm}^{3+}$ co-doped ZBYA microsphere laser was shown in Fig. 10.

The demonstration of ZBYA microsphere laser devices have shown that ZBYA glass material can be a good candidate for lasing applications. The realization of C-band and S-band lasers also shows the potential of ZBYA microspheres for use in the optical communications field.

3.3. MIR Fiber lasers in ZBYA glass fiber

Over the past few decades, MIR fiber lasers have received widespread research interest due to their extensive applications in environmental monitoring, biomedicine, military applications

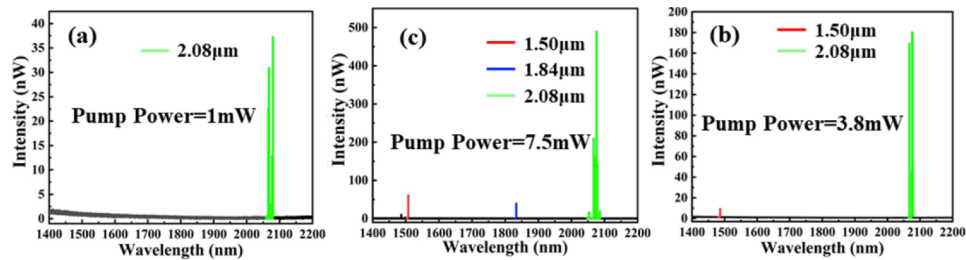


Fig. 10. Laser spectrum at varying pump power (a) 1 mW, (b) 3.8 mW, (c) 7.5 mW [47].

and other areas [48–51]. To further explore the potential of ZBYA glass to implement high power mid-infrared lasers, we have recently fabricated single-cladding ZBYA glass fibers. Ho^{3+} -doped ZBYA glass fiber was prepared by the suction method and used as a gain medium to build the fiber laser. Due to the severe tendency of fluoride glasses to crystallize, rapid cooling is essential in the preparation of the preform to very quickly reduce the glass from high temperature to below the glass transition temperature. The core and cladding glass components are $50\text{ZrF}_4\text{-}33\text{BaF}_2\text{-}6.5\text{YF}_3\text{-}7\text{AlF}_3\text{-}2\text{PbF}_2\text{-}1.5\text{HoF}_3$ and $50\text{ZrF}_4\text{-}33\text{BaF}_2\text{-}10\text{YF}_3\text{-}7\text{AlF}_3$ respectively, the corresponding refractive indices are 1.511 and 1.499 at 2.0 μm . The background loss of Ho^{3+} doped ZBYA glass fibers was measured by the cut-back method, resulting in an attenuation value of 1.0 dB/m at 1570 nm. There are two main sources of background loss: scattering loss caused by the uneven density of the preform that arises during condensation, and the absorption caused by impurities in the raw materials.

In order to test the 2.9 μm laser performance of Ho^{3+} doped ZBYA glass fiber, we constructed a forward-pumped laser device as depicted in Fig. 11. The core and cladding diameters of the Ho^{3+} doped ZBYA glass fiber were 20 μm and 250 μm , respectively. A 1150 nm Raman fiber laser was used as the pump source, and the 1150 nm laser is coupled into the 24 cm ZBYA gain fiber after passing through a focusing lens and a dichroic mirror (high transmittance at 1150 nm and high reflectivity at $\sim 2.9 \mu\text{m}$). Before the power meter, a 2400 nm long-wave passband filter was used to filter out residual pump light.

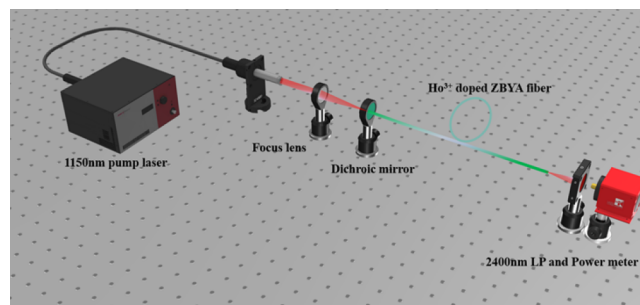


Fig. 11. Experimental setup of the ZBYA glass fiber laser at $\sim 2.9 \mu\text{m}$.

Figure 12(a) displays the variation laser output power at $\sim 2.9 \mu\text{m}$ as a function of the launched pump power when the gain fiber length was 24 cm. A minimum laser output power of 12 mW was obtained when the corresponding launched pump power was 72.5 mW. The laser threshold may be less than 72.5 mW, but power pump power levels were limited by the minimum power setting adjustment interval of the 1150 nm pump laser. The maximum output power of 762.8 mW was achieved for a launched pump power of 3.96 W, and the slope efficiency was 19.6%. Figure 12(b) shows the laser spectrum at different output powers of 12 mW, 18 mW and 680 mW which was

measured with an optical spectrum analyzer (YOKOGAWA AQ6377). Single wavelength lasing (2862 nm) was obtained when the output power was 12 mW, and the multi-wavelength lasing was excited when the output power was increased to 18 mW. Multi-wavelength laser operation is mainly due to the spectral characteristics of the dichroic mirror (DM) used in the experiment, which has high broadband reflectivity at $\sim 2.9 \mu\text{m}$. As the pump power increases, the gain of the different laser spectral lines becomes higher than the cavity loss, resulting in multi-wavelength laser operation.

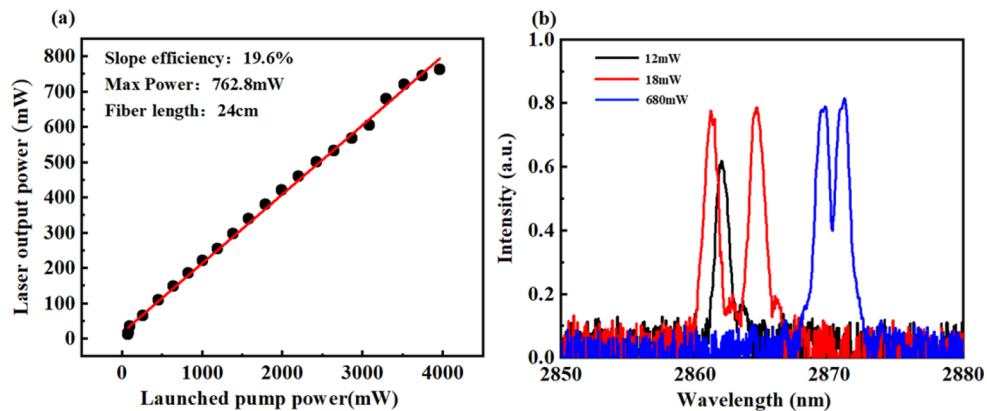


Fig. 12. (a) Output power at $\sim 2.9 \mu\text{m}$ in the 24 cm long gain fiber with respect to the launched pump power and (b) laser spectrum at different output power.

4. Conclusion

This paper reviews the luminescence properties of ZBYA glass in the MIR band and its applications as a laser gain medium in microsphere and fiber lasers. Due to the low phonon energy and good physical properties, ZBYA glass has unique advantages in MIR laser applications. Furthermore, it is worth noting that the optical resonance occurring in the whispering gallery mode microsphere cavity is very sensitive to changes in the external environment, allowing the use of ZBYA glass microsphere resonators in a variety of sensing applications, such as temperature sensing, pressure sensing, electromagnetic field sensing, refractive index sensing, gas sensing and biological sensing. For a ZBYA glass fiber laser, the fiber manufacturing processes need to be optimized and the purity of the raw materials needs to be improved to reduce the background loss in the gain fiber. In order to lessen the complexity of laser system and increase the maximum pump power, the replacement of the DM in the laser cavity with a Fiber Bragg Grating (FBG), inscribed directly in the ZBYA gain fiber, is a priority for future development of the laser. Further research will concentrate on the fabrication of double-cladding ZBYA glass fiber in order to apply ZBYA glass fibers to high power mid-infrared laser systems.

Funding. National Natural Science Foundation of China (61905048, 61935006, 62005060, 62005061, 62090062); Heilongjiang Provincial Natural Science Foundation (LH2020F030); National Key Research and Development Program of China (2020YFA0607602); Shenzhen Basic Research Foundation (JCYJ20190808140805488, JCYJ20190808173619062); 111 Project (B13015); Heilongjiang Touyan Innovation Team Program; Fundamental Research Funds for the Central Universities (3072021CF2514, 3072021CF2533).

Disclosures. The authors declare no conflicts of interest

Data availability. Data underlying the results presented in this paper are not publicly available at this time but may be obtained from the authors upon reasonable request

References

1. E. Snitzer, "Optical laser action of Nd^{3+} in a barium crown glass," *Phys. Rev. Lett.* **7**(12), 444–446 (1961).

2. A. M. Efimov and V. G. Pogareva, "Water-related IR absorption spectra for some phosphate and silicate glasses," *J. Non-Cryst. Solids* **275**(3), 189–198 (2000).
3. L. Gomes, J. Lousteau, D. Milanese, E. Mura, and S. D. Jackson, "Spectroscopy of mid-infrared (2.9 μm) fluorescence and energy transfer in Dy^{3+} -doped tellurite glasses," *J. Opt. Soc. Am. B* **31**(3), 429–435 (2014).
4. Y. Lu, M. Cai, R. Cao, S. Qian, S. Xu, and J. Zhang, " Er^{3+} doped germanate–tellurite glass for mid-infrared 2.7 μm fiber laser material," *J. Quant. Spectrosc. Radiat. Transfer* **171**, 73–81 (2016).
5. K. Yoshimoto, Y. Ezura, M. Ueda, A. Masuno, and H. Inoue, "2.7 μm Mid-Infrared Emission in Highly Erbium-Doped Lanthanum Gallate Glasses Prepared Via an Aerodynamic Levitation Technique," *Adv. Opt. Mater.* **6**(8), 1701283 (2018).
6. M. J. Weber, J. D. Myers, and D. H. Blackburn, "Optical properties of Nd^{3+} in tellurite and phosphotellurite glasses," *J. Appl. Phys.* **52**(4), 2944–2949 (1981).
7. M. Poulain, M. Poulain, and J. Lucas, "Verres fluores au tetrafluorure de zirconium proprietes optiques d'un verre dope au Nd^{3+} ," *Mater. Res. Bull.* **10**(4), 243–246 (1975).
8. W. L. Vaughn and S. H. Risbud, "New fluoronitride glasses in zirconium-metal-F-N systems," *J. Mater. Sci. Lett.* **3**(2), 162–164 (1984).
9. M. Poulain, "Halide glasses," *J. Non-Cryst. Solids* **56**(1-3), 1–14 (1983).
10. H. Ebendorff-Heidepriem, I. Szabó, and Z. E. Rasztovtovits, "Crystallization behavior and spectroscopic properties of Ho^{3+} -doped ZBYA-fluoride glass," *Opt. Mater.* **14**(2), 127–136 (2000).
11. E. H. Penilla, L. F. Devia-Cruz, M. A. Duarte, C. L. Hardin, Y. Kodera, and J. E. Garay, "Gain in polycrystalline Nd-doped alumina: leveraging length scales to create a new class of high-energy, short pulse, tunable laser materials," *Light: Sci. Appl.* **7**(1), 33 (2018).
12. C. Yao, Z. Jia, Z. Li, S. Jia, Z. Zhao, L. Zhang, Y. Feng, G. Qin, Y. Ohishi, and W. Qin, "High-power mid-infrared supercontinuum laser source using fluorotellurite fiber," *Optica* **5**(10), 1264 (2018).
13. J. Bei, H. T. C. Foo, G. Qian, T. M. Monro, A. Hemming, and H. Ebendorff-Heidepriem, "Experimental study of chemical durability of fluorozirconate and fluoroindate glasses in deionized water," *Opt. Mater. Express* **4**(6), 1213–1226 (2014).
14. C. Xu, J. Zhang, X. Zhao, H. Zhao, F. Ling, S. Jia, G. Farrell, S. Wang, and P. Wang, "Two-watt mid-infrared laser emission in robust fluorozirconate fibers," *Opt. Lett.* **47**(6), 1399–1402 (2022).
15. C. J. Simmons and J. H. Simmons, "Chemical durability of fluoride glasses: I, reaction of fluorozirconate glasses with water," *J. Am. Ceram. Soc.* **69**(9), 661–669 (1986).
16. J. Lucas, "Fluoride glasses," *J. Mater. Sci.* **24**(1), 1–13 (1989).
17. T. Iqbal, M. R. Shahriari, G. Merberg, and G. H. Sigel, "Synthesis, characterization, and potential application of highly chemically durable glasses based on AlF_3 ," *J. Mater. Res* **6**(2), 401–406 (1991).
18. F. Huang, Y. Ma, W. Li, X. Liu, L. Hu, and D. Chen, "2.7 μm emission of high thermally and chemically durable glasses based on AlF_3 ," *Sci. Rep.* **4**(1), 3607 (2015).
19. F. Gan, "Optical properties of fluoride glasses: a review," *J. Non-Cryst. Solids* **184**, 9–20 (1995).
20. L. Wetenkamp, G. F. West, and H. Többen, "Optical properties of rare earth-doped ZBLAN glasses," *J. Non-Cryst. Solids* **140**, 35–40 (1992).
21. C. R. Day, P. W. France, S. F. Carter, M. W. Moore, and J. R. Williams, "Overview of fluoride glass fiber optics," *New Materials for Optical Waveguides* (SPIE, 1987), Vol. 0799, pp. 94–100.
22. X. Zhu and N. Peyghambarian, "High-power ZBLAN glass fiber lasers: review and prospect," *Adv. Optoelectron.* **2010**, 1–23 (2010).
23. F. Huang, Y. Guo, Y. Ma, L. Zhang, and J. Zhang, "Highly Er^{3+} -doped ZrF_4 -based fluoride glasses for 2.7 μm laser materials," *Appl. Opt.* **52**(7), 1399–1403 (2013).
24. F. Huang, X. Liu, W. Li, L. Hu, and D. Chen, "Energy transfer mechanism in Er^{3+} doped fluoride glass sensitized by Tm^{3+} or Ho^{3+} for 2.7 μm emission," *Chin. Opt. Lett.* **12**(5), 051601 (2014).
25. F. Huang, Y. Tian, S. Xu, and J. Zhang, "Spectroscopic and energy transfer mechanism of Er^{3+} , Pr^{3+} -codoped ZBYA glass," *Ceram. Int.* **42**(7), 7924–7928 (2016).
26. S. W. Deng, T. F. Xu, X. Wang, S. X. Dai, X. Shen, G. X. Wang, and Q. H. Nie, "Preparation and the mid-infrared emission properties of $\text{Dy}^{3+}/\text{Tm}^{3+}$ -codoped $\text{GeS}_2\text{-Ga}_2\text{S}_3\text{-PbI}_2$ glasses," *J. Optoelectron. Laser* **22**, 223–227 (2011).
27. H. Zhao, S. Jia, X. Wang, R. Wang, X. Lu, Y. Fan, M. Tokurakawa, G. Brambilla, S. Wang, and P. Wang, "Investigation of $\text{Dy}^{3+}/\text{Tm}^{3+}$ co-doped $\text{ZrF}_4\text{-BaF}_2\text{-YF}_3\text{-AlF}_3$ fluoride glass for efficient 2.9 μm mid-infrared laser applications," *J. Alloys Compd.* **817**, 152754 (2020).
28. H. Zhao, R. Wang, X. Wang, S. Jia, Y. Fan, Y. Fan, E. Lewis, G. Farrell, S. Wang, S. Wang, P. Wang, P. Wang, and P. Wang, "Intense mid-infrared emission at 3.9 μm in Ho^{3+} -doped ZBYA glasses for potential use as a fiber laser," *Opt. Lett.* **45**(15), 4272–4275 (2020).
29. P. Wang, G. S. Murugan, G. Brambilla, M. Ding, Y. Semenova, Q. Wu, and G. Farrell, "Chalcogenide microsphere fabricated from fiber tapers using contact with a high-temperature ceramic surface," *IEEE Photonics Technol. Lett.* **24**(13), 1103–1105 (2012).
30. C. Y. Chao and L. J. Guo, "Biochemical sensors based on polymer microrings with sharp asymmetrical resonance," *Appl. Phys. Lett.* **83**(8), 1527–1529 (2003).

31. D. Rafizadeh, J. P. Zhang, S. C. Hagness, A. Taflove, K. A. Stair, S. T. Ho, and R. C. Tiberio, "Waveguide-coupled AlGaAs/GaAs microcavity ring and disk resonators with high finesse and 21.6-nm free spectral range," *Opt. Lett.* **22**(16), 1244–1246 (1997).
32. M.-C. M. Lee and M. C. Wu, "MEMS-actuated microdisk resonators with variable power coupling ratios," *IEEE Photonics Technol. Lett.* **17**(5), 1034–1036 (2005).
33. D. K. Armani, T. J. Kippenberg, S. M. Spillane, and K. J. Vahala, "Ultra-high-Q toroid microcavity on a chip," *Nature* **421**(6926), 925–928 (2003).
34. D. Armani, B. Min, A. Martin, and K. J. Vahala, "Electrical thermo-optic tuning of ultrahigh-Q microtoroid resonators," *Appl. Phys. Lett.* **85**(22), 5439–5441 (2004).
35. G. S. Murugan, J. S. Wilkinson, and M. N. Zervas, "Selective excitation of whispering gallery modes in a novel bottle microresonator," *Opt. Express* **17**(14), 11916–11925 (2009).
36. G. S. Murugan, M. N. Petrovich, Y. Jung, J. S. Wilkinson, and M. N. Zervas, "Hollow-bottle optical microresonators," *Opt. Express* **19**(21), 20773–20784 (2011).
37. S. Berneschi, D. Farnesi, F. Cosi, G. N. Conti, S. Pelli, G. C. Righini, and S. Soria, "High Q silica microbubble resonators fabricated by arc discharge," *Opt. Lett.* **36**(17), 3521–3523 (2011).
38. M. Cai, O. Painter, K. J. Vahala, and P. C. Sercel, "Fiber-coupled microsphere laser," *Opt. Lett.* **25**(19), 1430–1432 (2000).
39. X. Peng, F. Song, S. Jiang, N. Peyghambarian, M. Kuwata-Gonokami, and L. Xu, "Fiber-taper-coupled L-band Er³⁺-doped tellurite glass microsphere laser," *Appl. Phys. Lett.* **82**(10), 1497–1499 (2003).
40. L. Peng, Y. Huang, Y. Duan, S. Zhuang, T. Liao, and C. Xu, "2 μm laser oscillation of Ho³⁺ Tm³⁺-codoped silica microspheres," *Appl. Opt.* **56**(26), 7469–7473 (2017).
41. G. R. Elliott, G. S. Murugan, J. S. Wilkinson, M. N. Zervas, and D. W. Hewak, "Chalcogenide glass microsphere laser," *Opt. Express* **18**(25), 26720–26727 (2010).
42. G. S. Murugan, M. N. Zervas, Y. Panitchob, and J. S. Wilkinson, "Integrated Nd-doped borosilicate glass microsphere laser," *Opt. Lett.* **36**(1), 73–75 (2011).
43. Z. Fang, S. N. Chormaic, S. Wang, X. Wang, J. Yu, Y. Jiang, J. Qiu, and P. Wang, "Bismuth-doped glass microsphere lasers," *Photonics Res.* **5**(6), 740–744 (2017).
44. J. M. Ward, D. G. O'Shea, B. J. Shortt, and S. N. Chormaic, "Optical bistability in Er-Yb codoped phosphate glass microspheres at room temperature," *J. Appl. Phys.* **102**(2), 023104 (2007).
45. H. Zhao, P. Wang, X. Wang, R. Wang, A. Li, W. Li, E. Lewis, Y. Fan, S. Jia, and S. Wang, "Up-conversion luminescence and C-band laser in Er³⁺-doped fluorozirconate glass microsphere resonator," *IEEE Photonics J.* **11**(6), 1–7 (2019).
46. H. Y. Zhao, A. Z. Li, Y. T. Yi, M. Tokurakawa, G. Brambilla, S. J. Jia, S. B. Wang, and P. F. Wang, "A Tm³⁺-doped ZrF₄-BaF₂-YF₃-AlF₃ glass microsphere laser in the 2.0 μm wavelength region," *J. Lumin.* **212**, 207–211 (2019).
47. H. Zhao, Y. Yi, X. Wang, A. Li, A. Yang, Z. Yang, Y. Fan, S. Jia, E. Lewis, G. Brambilla, S. Wang, and P. Wang, "Triple-wavelength lasing at 1.50 μm , 1.84 μm and 2.08 μm in a Ho³⁺/Tm³⁺ co-doped fluorozirconate glass microsphere," *J. Lumin.* **219**, 116889 (2020).
48. H. Pratisto, M. Frenz, M. Ith, V. Romano, D. Felix, R. Grossenbacher, H. J. Altermatt, and H. P. Weber, "Temperature and pressure effects during erbium laser stapedotomy," *Lasers Surg. Med.* **18**(1), 100–108 (1996).
49. M. Frenz, H. Pratisto, F. Konz, E. D. Jansen, A. J. Welch, and H. P. Weber, "Comparison of the effects of absorption coefficient and pulse duration of 2.12 μm and 2.79 μm radiation on laser ablation of tissue," *IEEE J. Quantum Electron.* **32**(12), 2025–2036 (1996).
50. D. D. Hudson, D. D. Hudson, S. Antipov, S. Antipov, L. Li, I. Alamgir, M. E. Amraoui, Y. Messaddeq, M. Rochette, S. D. Jackson, A. Fuerbach, and A. Fuerbach, "Octave-spanning supercontinuum in the mid-IR with a 3 μm ultrafast fiber laser," *Nonlinear Optics, NTu3A.3* (2017).
51. B. Jean and T. Bende, "Mid-IR laser applications in medicine," *Topics in Applied Physics* **89**, 511–544 (2003).